Available online at www.sciencedirect.com
SCIENCE DIRECT®
Journal of Magnetic Resonance 164 (2003) 78–83
JMR Journal of Magnetic Resonance
www.elsevier.com/locate/jmr

Improving W-band pulsed ENDOR sensitivity—random acquisition and pulsed special TRIPLE

B. Epel, D. Arieli, D. Baute, and D. Goldfarb*

Department of Chemical Physics, Weizmann Institute of Science, Rehovot 76100, Israel

Received 17 February 2003; revised 4 June 2003

Abstract

Two approaches for improving the signal-to-noise ratio (S/N) of W-band pulsed electron-nuclear double resonance (ENDOR) spectra are presented. One eliminates base-line problems while the other enhances the ENDOR effect. High field ENDOR spectra measured at low temperatures often suffer from highly distorted base-lines due to the heating effect of the RF pulses that causes some detuning of the cavity and therefore leads to a reduction in the echo intensity. This is a severe problem because it often masks broad and weak ENDOR signals. We show that it can be eliminated by recording the ENDOR spectrum in a random, rather than the standard sequential variation of the RF frequency. The S/N of the ENDOR spectrum can be significantly enhanced by the application of the pulse analog of the continuous wave (CW) special TRIPLE experiment. While this experiment is not applicable in the solid state at conventional X-band frequencies, at W-band it is most efficient. We demonstrate the efficiency of the special TRIPLE Davies and Mims experiments on single crystals and orientationally disordered systems.
© 2003 Elsevier Inc. All rights reserved.

1. Introduction

Pulsed electron-nuclear double resonance (ENDOR) spectroscopy has become a well established technique for the determination of the spatial and electronic structure of paramagnetic entities. While the most frequently used pulse experiments are the Davies [1] and Mims [2] ENDOR sequences, in the last 10–15 years a number of new pulse ENDOR sequences, aimed at improving the signal-to-noise ratio (S/N), enhancing resolution and facilitating signal assignment, were introduced. These are described in details in the review of Gemperle and Schweiger [3] and the recent book of Schweiger and Jeschke [4]. The double resonance has been extended to triple resonance experiments such as hyperfine selective ENDOR [5], TRIPLE [6], and quadruple resonance [7]. The first two have also been expanded into two-dimensional experiments [3,8]. In parallel to these new experimental methodologies, the recent development of high field ENDOR has introduced many additional advantages [9–12].

One feature shared by all forms of the ENDOR technique is that they are difference experiments, namely, a particular sequence of microwave pulses generates an echo and the effect of the RF pulse(s) on its intensity is measured. An example is the Davies ENDOR sequence shown in Fig. 1a. The ENDOR effect is defined according to [4]:

$$F_{\mathrm{ENDOR}} = \frac{1}{2}\frac{I(\mathrm{off}) - I(\mathrm{on})}{I(\mathrm{off})}, \tag{1}$$

where $I(\mathrm{on})$ and $I(\mathrm{off})$ correspond to the echo intensity with and without the RF pulse(s), respectively. The TRIPLE sequence [6], shown in Fig. 1b, is actually a "double" difference experiment, where the difference in the ENDOR effect is followed as a function of a second RF pulse.

Most often the ENDOR effect is weak, and although the echo itself may be intense, the observation of the ENDOR spectrum requires long signal averaging. Moreover, the difference nature of the experiment makes it highly susceptible to very small fluctuations (instabilities) in magnetic field, frequency, phase, etc. Consequently, S/N problems are always of major concern. Improvement in the S/N can be achieved by optimizing

* Corresponding author. Fax: +972-8-934-4123.
E-mail address: daniella.goldfarb@weizmann.ac.il (D. Goldfarb).

1090-7807/$ - see front matter © 2003 Elsevier Inc. All rights reserved.
doi:10.1016/S1090-7807(03)00191-5

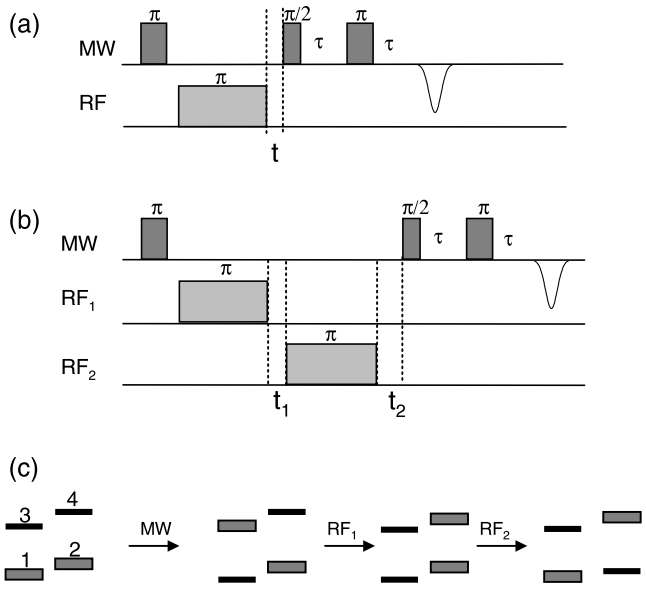

Fig. 1. (a) The Davies ENDOR pulse sequence, (b) the TRIPLE sequence and of the corresponding evolution of the populations.

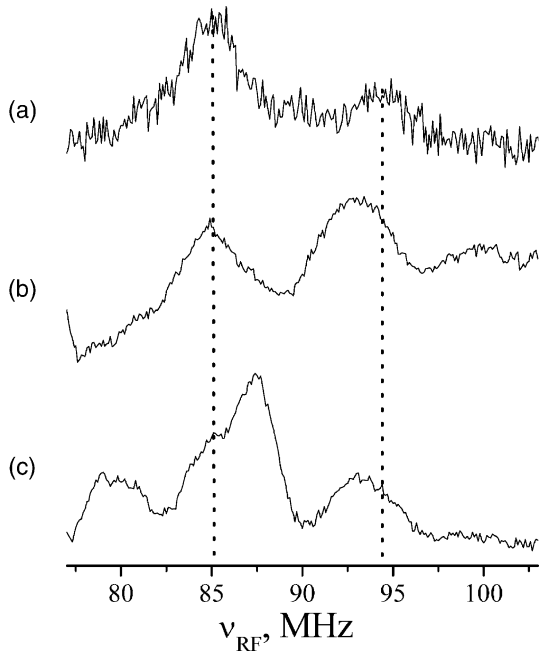

Fig. 2. (a) Davies ENDOR spectrum (random acquisition) of Mn-UCSB-6Mg ($\tau = 0.4\,\mu s$, $t_{RF} = 10\,\mu s$, $t = 5\,\mu s$, 45 scans, and repetition time (t_{rep}) of 8 ms). (b) Same as (a) with normal acquisition, (c) same as (b) with $t_{rep} = 4$ ms (13 scans). Other experimental conditions for all spectra: microwave pulse lengths: 0.07, 0.035, 0.07 μs; $T = 5$ K; $B_0 = 3.39$ T; 30 shots per point. The dotted lines mark the two ^{55}Mn ENDOR lines.

the technical performance of the spectrometer on one hand, and by designing experiments that have a larger ENDOR effect on the other. Here we present two methods for acquiring ENDOR spectra that result in a significant improvement in the S/N. The first is the "random" acquisition of the ENDOR spectrum, which removes base-line problems due to RF induced heating. The second is the pulse analog of the CW Special TRIPLE experiment, which enhances the ENDOR effect by a factor of two and is applicable mostly at high fields.

2. Results and discussion

2.1. Random acquisition

The majority of pulse ENDOR experiments are carried out at low temperatures; for nitroxide and other organic radicals liquid nitrogen cooling is sufficient, whereas paramagnetic transition metal ions call for temperatures in the range of 1.2–15 K, obtained with liquid He cooling. This introduces new complications because, in addition to the desired field and frequency stability, the temperature and He flow stabilities become of major importance. At high frequencies, such as 95 GHz, the cavity tuning and the phase of the signal are highly sensitive to subtle changes in the temperature/He flow. Consequently, in addition to the desired resonance effect, the RF pulse usually also causes undesirable local heating that results in detuning and leads to an additional decrease in the echo intensity. If the intensity profile of the applied RF is not constant (as is usually the case) this effect manifests itself as a base-line with broad humps (see, for example, Fig. 2b,c), which interferes with the observation of the ENDOR effect. This is particularly problematic in the case of broad peaks or powder patterns and/or very weak ENDOR effects. Signal averaging does not alleviate this problem because the heating effect within a certain RF range and experimental conditions is constant and reproducible and will, therefore, just build up along with the signal. Similarly, phase cycling that is often the remedy for base-line drift will not be effective in this case since the effect has the same sensitivity to the phase as the echo. One approach to solve this problem is constructing a feedback loop that will level the RF power profile such that the power felt by the sample is constant within the range scanned. This would have to take into account both the profiles of the amplifier power and the RF coil, which is not a trivial task in terms of the hardware set-up. A simpler and cheaper approach is to change the way the ENDOR spectrum is acquired through the software.

Usually the ENDOR spectrum is acquired by incrementally changing the frequency of the RF pulse according to:

$$\nu_{RF}(i) = \nu_{RF}(1) + d\mathrm{RF}(i-1), \quad (2)$$

where $\nu_{RF}(1)$ is the starting frequency, dRF is the frequency step, and i is incrementally changed from 1 to npt

such that the total scanned range is $\Delta RF = dRF \cdot npt$, and *npt* is the total number of points. This same scheme is repeated in each scan thus generating the same heating profile. However, if i is varied randomly, rather than sequentially, the heating profile of each scan is different and the base-line problems are eliminated through averaging. A somewhat similar approach was reported in CW ENDOR experiments by Brüggemann and Niklas [13], which was referred to as stochastic ENDOR. In this case, however, the arbitrarily chosen radio frequency aimed at overcoming problems arising from low RF modulation frequencies required for nuclei with very long spin–lattice relaxation times, which results in very low S/N. Nonetheless, this method also leads to a better noise immunity.

All ENDOR spectra presented in this communication were recorded on a home built W-band (95 GHz) spectrometer [11], which is controlled by a new, highly versatile software, *SpecMan* [14], we recently developed together with the group of A. Schweiger at the ETH, Zurich. For each frequency $\nu_{RF}(i)$, n shots are acquired (typically $n = 30$) and summed by the boxcar integrator, then the next frequency value is selected until a full scan is completed. This is repeated for a large number of scans, required for averaging the noise (base-line humps) induced by the RF heating. In principle, in order for the averaging to be more efficient, it is better to reduce the number of shots and increase the number of scans. The frequency change does not require any special attention and is carried out just as in the sequential acquisition. The random acquisition method was first tested by comparing room temperature ^{1}H ENDOR spectrum of a standard acquired in the conventional sequential way and by random acquisition. The heating effect at room temperature is negligible and therefore there are no base-line problems. As expected, no differences between the spectra were observed (data not shown).

Fig. 2 shows W-band Davies ENDOR spectra of a polycrystalline sample of Mn(II) incorporated into an aluminophosphate molecular sieve, Mn-UCSB-6Mg [15]. It displays the region of 77–103 MHz, where the ^{55}Mn ENDOR lines of the Mn(II) $M_S = -1/2$ manifold are expected [16]. The spectrum shown in Fig. 2a was obtained with random acquisition; the base-line is flat and two ENDOR peaks, marked with dotted lines, are easily detected. The two peaks correspond to two Mn(II) centers with different ^{55}Mn hyperfine couplings. The trace shown in Fig. 2b, which was acquired under the same conditions using the normal sequential approach, is dominated by a base–line with intense humps masking the ENDOR signal. These humps depend on experimental conditions such as the RF pulse length, repetition rate, or number of shots. For example, the trace shown in Fig. 2c was acquired using the standard method and the same conditions as Fig. 2b, yet, the repetition rate was twice as fast. The 'new' base-line detected in Fig. 2c shows that the humps observed in the standard acquisition are indeed not ENDOR signals. The noise in the randomly acquired spectrum (Fig. 2a) appears at first glance higher than in the other traces, but one should recall that the amplitude of the humps is part of the noise.

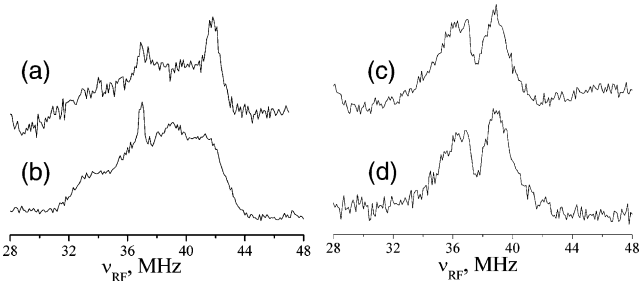

Fig. 3. Davies ENDOR spectra of two sulfur centered radicals trapped in sodalite: (a) Radical I (normal acquisition; $B_0 = 3.33$ T, $\tau = 0.3$ μs, $t_{RF} = 12$ μs, 10 scans, and $t_{rep} = 5$ ms). (b) Same as (a) with random acquisition ($\tau = 0.4$ μs, $t_{RF} = 10$, 80 scans, and $t_{rep} = 8$ ms). (c) Radical II (normal acquisition; $B_0 = 3.32$ T, $\tau = 0.4$ μs, $t_{RF} = 10$ μs, 38 scans, and $t_{rep} = 8$ ms). (d) Same as (c) with random acquisition. Other experimental conditions for all spectra: MW pulse lengths 0.2, 0.1, 0.2 μs; $t = 5$ μs, $T = 4.5$–5.6 K; 30 shots per point.

Another example of the effectiveness of the random acquisition is shown in Fig. 3. Fig. 3a presents the sequentially acquired Davies ENDOR spectrum of a sulfur centered radical, radical I, trapped in the cage of the zeolite sodalite. The spectrum is dominated by a distorted base-line and it is difficult to distinguish between the base-line and the signal. Fig. 3b is a Davies ENDOR spectrum acquired by the random acquisition method; in addition to the narrow signals close to the ^{27}Al Larmor frequency, a superposition of two broad ^{23}Na doublets with splittings of about 3 and 8 MHz are clearly detected. Figs. 3c and d compare the normal and random Davies ENDOR, respectively, of another sulfur centered radical trapped in the sodalite cage, radical II, prepared under different conditions. In this case only the doublet associated with the smaller ^{23}Na hyperfine (~3 MHz) appears and the base-line distortion is significantly less dramatic because the signal is narrower and the ENDOR effect is larger.

2.2. Special TRIPLE

In continuous wave (CW) ENDOR experiments the ENDOR effect is significantly enhanced by the application of the special TRIPLE experiment [17,18]. This technique requires the saturation of the NMR transitions in both electron spin manifolds and it works only when the relation between the two transition frequencies is known. In liquid samples, where the hyperfine interaction is isotropic, the two NMR transitions are symmetric with respect to the Larmor frequency, ν_I (weak

coupling case). Consequently, the special TRIPLE experiment is implemented by scanning two RF frequencies simultaneously and symmetrically about ν_I of the nucleus of interest, i.e., one frequency decreases towards $\nu_I - \Delta RF/2$, while the other increases towards $\nu_I + \Delta RF/2$.

The pulse version of the special TRIPLE experiment has been previously proposed [3,19]; it is similar to the pulse TRIPLE experiment [6], the difference being the way the frequency of the two RF pulses is scanned. While in the normal (or general) TRIPLE experiment one RF frequency is set on resonance with an ENDOR transition and the frequency of the other RF pulse is scanned, in the special TRIPLE the frequencies of the two RF pulses are scanned simultaneously as in the CW experiment. The evolution of the populations during the experiment is shown in Fig. 1c for a simple four level system of $S = 1/2, I = 1/2$. The first MW π pulse inverts the population of the 1–3 EPR transition, whereas the first RF π pulse inverts the population of the 3–4 NMR transition, thus equalizing the 1–3 populations. This is the stage of signal detection in the Davies ENDOR experiment and the maximum ENDOR effect is 0.5 (Eq. (1)). The second RF π pulse, on-resonance with the 1–2 NMR transition, inverts the corresponding populations, resulting in a positive polarization of the 1–3 EPR transition and, therefore, the final echo detection will give a maximum ENDOR effect of 1. This is a rather simple experiment; its only crucial requirement is that the RF pulses are simultaneously on resonance with the two NMR transitions of the $M_S = \pm 1/2$ manifolds. The reason this experiment has not been realized experimentally so far [3] is that pulsed ENDOR is generally applicable for solid samples, where, at X-band frequencies, the NMR transitions are not exactly symmetric about ν_I. Accordingly, if the frequency of one of the NMR transitions is known, the corresponding transition in the other manifold is still unknown. To overcome this problem, Gemperle et al. [19] have proposed an alternative experiment where an additional MW π pulse is inserted between the two RF pulses, both having the same frequency. The theoretical enhancement is a factor of two, similar to that of the special TRIPLE, however, the introduction of a second π pulse is problematic and leads to additional signal losses. Hence, this experiment is not frequently used.

In contrast to X-band frequencies, at high frequencies such as W-band, the two NMR frequencies are usually symmetric about ν_I, also for solids, and the special TRIPLE experiment is most useful. We first demonstrate it on the ^{1}H spectrum of a single crystal of Cu(II)-doped L-histidine where the ENDOR lines are very narrow (see Fig. 4). The dotted line represents the normal Davies ENDOR spectrum, the solid line shows the special TRIPLE spectrum, for which the ENDOR effect is indeed double. Note that only one half of the spectrum is obtained. In the TRIPLE experiment the echo intensity is reduced relative to that of the standard ENDOR experiment due to the additional electron spin relaxation that takes place during the time of the second RF pulse. Although this does not affect the ENDOR effect, as shown in Fig. 4, it can affect to some extent the S/N if the echo decay is appreciable.

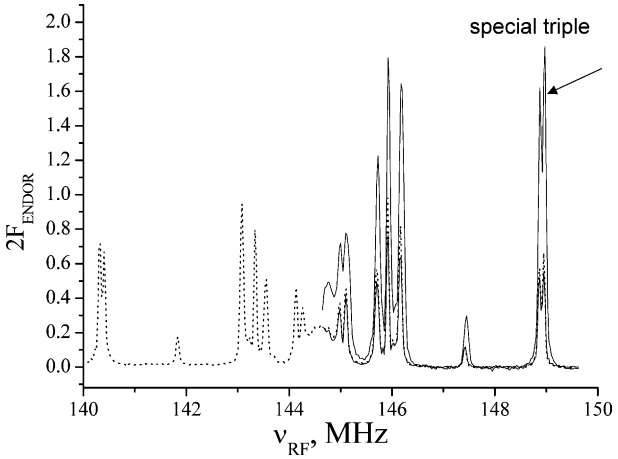

Fig. 4. Spectra of a single crystal of Cu(II)-doped L-histidine. Dotted trace: Davies ENDOR, $t = 5\,\mu s$. Solid trace (low intensity) Davies ENDOR, $t = 20\,\mu s$. Solid trace (high intensity): special TRIPLE, $t_1 = 0.2\,\mu s$, $t_2 = 5\,\mu s$. Other experimental conditions for all spectra: MW pulse length: 0.2, 0.1, and 0.2 μs, $\tau = 2\,\mu s$, $T = 8\,K$; $B_0 = 3.393\,T$; $t_{RF} = 15\,\mu s$; $t_{rep} = 10\,ms$, 30 shots per point, one scan. (A very long τ was used to reduce the echo intensity and avoid saturation of the detection system.) All spectra were acquired with normal acquisition.

A comparison between the ENDOR effect in Davies ENDOR and special TRIPLE for an orientationally disordered system, a frozen solution of a Cu(II)–(histidine)$_2$ in D_2O (1 mM, pH = 7.3), is shown in Fig. 5a. Although the ^{1}H ENDOR effect is significantly lower than in the single crystal, the almost twofold increase in the ENDOR effect in the special TRIPLE experiment is clear. In this case both spectra were collected using the random acquisition method where the same randomization was used for the two RF pulses in each scan. Finally, we present the ^{13}C ENDOR/special TRIPLE of a frozen solution of a Cu(II) complex (1 mM, pH = 3.8). When the Davies ENDOR was collected by sequential acquisition it was not possible to observe the ^{13}C lines due to base-line distortions that masked the weak ENDOR effect. The asymmetry in the intensity of the doublet is due to a partial saturation of the NMR transitions [20]. In principle, this asymmetry could be removed without changing the repetition rate, by reducing the number of shots per RF point to 1 and performing the signal averaging by increasing the number of scans. The special TRIPLE spectrum again shows a stronger ENDOR effect. Note the significantly lower number of scans in the special TRIPLE experiment.

The special TRIPLE experiment applies also to Mims ENDOR, where two RF pulses are introduced during

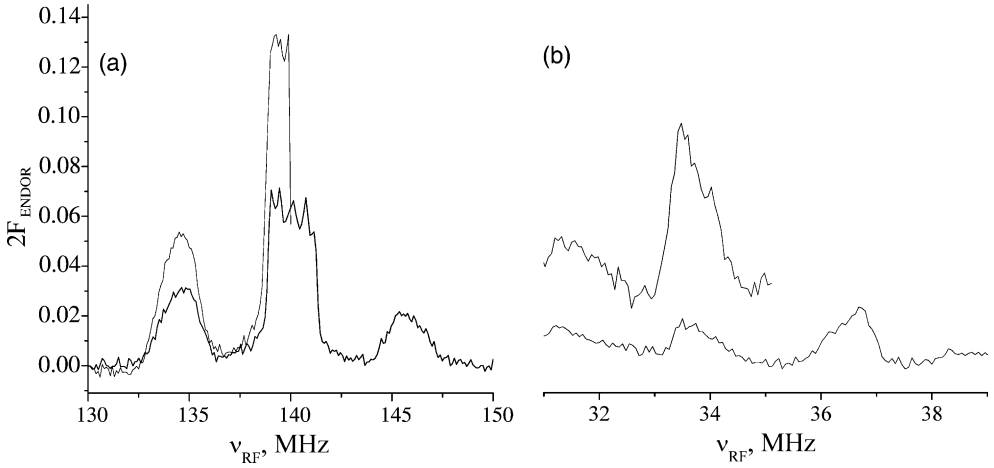

Fig. 5. (a) ^{1}H ENDOR spectra of a frozen solution of Cu(II)–(histidine)$_2$ (1 mM, pH = 7.3 in D_2O). Bottom trace: Davies ENDOR ($t = 4\,\mu s$), Top trace: special TRIPLE ($t_1 = 1\,\mu s$, $t_2 = 4\,\mu s$). Other experimental conditions for top and bottom spectra: MW pulse length: 0.2, 0.1, and 0.2 μs, $\tau = 0.4\,\mu s$, $t_{RF} = 15\,\mu s$, $t_{rep} = 8\,ms$, 30 shots per point, 30 scans, $T = 6\,K$, $B_0 = 3.284\,T$, (b) W-band spectra of a frozen solution of Cu(II)–(1-[^{13}C]histidine)$_2$ at pH 3.9. Bottom trace: ^{13}C Davies ENDOR ($t = 8\,\mu s$, $t_{rep} = 8\,ms$, 208 scans). Top trace: special TRIPLE ($t_1 = 1\,\mu s$, $t_2 = 5\mu s$, $t_{rep} = 8\,ms$, 123 scans). Other experimental conditions for top and bottom spectra: MW pulse lengths: 0.2, 0.1, and 0.2 μs, $\tau = 0.42\,\mu s$, $B_0 = 3.279\,T$, $t_{RF} = 32\,\mu s$, 30 shots per point, $T = 7.3\,K$. All spectra were acquired with random acquisition.

the time interval between the second and third MW pulses and are scanned as in the Davies special TRIPLE version. This is demonstrated in Fig. 6, which compares the ^{19}F ENDOR effect of the standard Mims experiment and the corresponding special TRIPLE carried out on an irradiated single crystal of LiF.

The choice between standard ENDOR and special TRIPLE depends primarily on the extent of echo decay during the additional time needed to insert the second RF pulse. In all the examples shown in this work this decay was relatively small. Naturally, the special TRIPLE is not applicable when the interest is in ENDOR spectra with asymmetric intensities, such as the one presented in Fig. 5b, or in the variable mixing time (VMT) ENDOR experiment [20,21], both designed to determine signs of hyperfine couplings at high fields. Similarly, the standard ENDOR is preferable in the case of high spin systems, where transitions other than the $|-1/2\rangle \rightarrow |+1/2\rangle$ manifold contribute to the spectrum and also when the couplings are very small and grouped around the Larmor frequency.

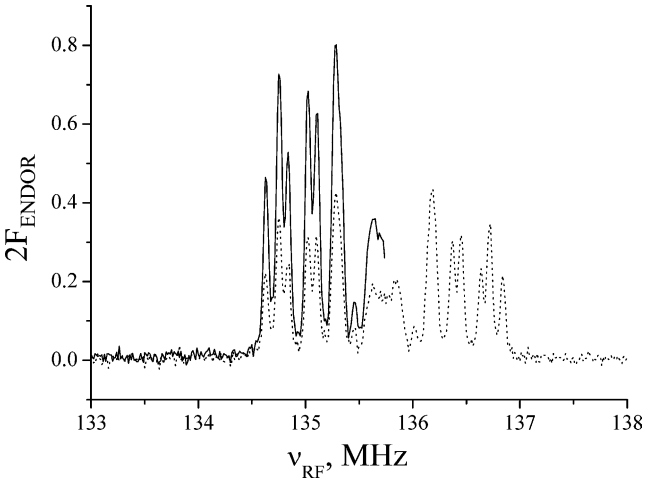

Fig. 6. ^{19}F spectra of a single crystal of irradiated LiF. Dotted trace: Mims ENDOR ($t = 35\,\mu s$). Solid trace: special TRIPLE Mims ($t_1 = 1\,\mu s$, $t_2 = 4\,\mu s$). Other experimental conditions for both spectra: MW pulse lengths: 0.06 μs, $\tau = 0.2\,\mu s$, $B_0 = 3.386\,T$, $t_{RF} = 30\,\mu s$, 30 shots per point, 1 scan, $T = 293\,K$, and $t_{rep} = 10\,ms$. All spectra were acquired with random acquisition.

Acknowledgments

This research was supported by the DFG Schwerpunkt program "High field EPR in Physics, Chemistry, and Biology." We are grateful to Dr. O. Poluektov for the preparation of the LiF sample.

References

[1] E.R. Davies, A new pulse ENDOR technique, Phys. Lett. 47A (1974) 1–2.
[2] W.B. Mims, Pulsed ENDOR experiments, Proc. R. Soc. Lond. A 283 (1965) 452–457.
[3] C. Gemperle, A. Schweiger, Pulsed electron-nuclear double resonance, Chem. Rev. 91 (1991) 1481–1505.
[4] A. Schweiger, G. Jeschke, Principles of Pulse Electron Paramagnetic Resonance, Oxford University Press, Oxford, 2001.
[5] H. Thomann, M. Bernardo, Pulsed electron nuclear electron triple resonance spectroscopy, Chem. Phys. Lett. 169 (1990) 5–11.
[6] M. Mehring, P. Höfer, A. Grupp, Pulsed electron nuclear double and triple resonance schemes, Ber. Bunseges. Phys. Chem. 91 (1987) 1132–1137.
[7] M.K. Bowman, A.M. Tyryshkin, Electron nuclear quadruple resonance for assignment of overlapping spectra, J. Magn. Reson. 144 (2000) 74–84.

[8] B. Epel, D. Goldfarb, Two-dimensional pulsed TRIPLE at 95 GHz, J. Magn. Reson. 146 (2000) 196–203.
[9] J.A.J.M. Disselhorst, H. van der Meer, O.G. Poluektov, J. Schmidt, A pulsed EPR and ENDOR spectrometer operating at 95 GHz, J. Magn. Reson. A 115 (1995) 183–188.
[10] T.F. Prisner, M. Rohrer, K. Möbius, Pulsed 95 GHz high-field EPR heterodyne spectrometer with high spectral and time resolution, Appl. Magn. Reson. 7 (1994) 167–183.
[11] I. Gromov, V. Krymov, P. Manikandan, D. Arieli, D. Goldfarb, A W-Band pulsed ENDOR spectrometer: setup and application to transition metal centers, J. Magn. Res. 139 (1999) 8–17.
[12] V. Weis, M. Bennati, M. Rossay, J.A. Bryant, R.G. Griffin, High field DNP and ENDOR with a novel multiple-frequency resonance structure, J. Magn. Reson. 140 (1999) 293–299.
[13] W. Brüggemann, J.R. Niklas, Stochastic ENDOR, J. Magn. Reson. A 108 (1994) 25–29.
[14] *SpecMan*, Weizmann Institute of Science, Israel and ETH, Switzerland, 2002.
[15] D. Arieli, A. Delabie, K.G. Strohmaier, D.E.W. Vaughan, D. Goldfarb, Isomorphous substitution of Mn(II) into aluminophosphate zeotypes: a combined high-field ENDOR and DFT study, J. Phys. Chem. B 106 (2002) 7509–7519.
[16] P. Manikandan, R. Carmieli, T. Shane, A.J. Kalb(Gilboa), D. Goldfarb, W-band ENDOR investigation of the manganese binding site of concanavalin A: determination of proton hyperfine couplings and their signs, J. Am. Chem. Soc. 122 (2000) 3488–3494.
[17] K.P. Dinse, R. Biehl, K. Möbius, Electron nuclear triple resonance of free radicals in solution, J. Chem. Phys. 61 (1974) 4335–4341.
[18] H. Kurreck, B. Kirste, W. Lubitz, Electron Nuclear Double Resonance Spectroscopy of Radicals in Solution, VCH Publishers, New York, 1988 (Chapter 3).
[19] C. Gemperle, O.W. Sørensen, A. Schweiger, R.R. Ernst, Optimized polarization transfer in pulsed ENDOR experiments, J. Magn. Reson. 87 (1990) 502–515.
[20] B. Epel, A. Pöppl, P. Manikandan, S. Vega, D. Goldfarb, J. Magn. Reson. 148 (2001) 388–397.
[21] M.T. Bennebroek, J. Schmidt, Pulsed ENDOR spectroscopy at large thermal spin polarizations and the absolute sign of the hyperfine interaction, J. Magn. Reson 128 (1997) 199–206.